Proceedings of DSCC2008
2008 ASME Dynamic Systems and Control Conference
October 20-22, 2008, Ann Arbor, Michigan, USA

DSCC2008-2212

CO-DESIGN OF A MEMS ACTUATOR AND ITS CONTROLLER USING FREQUENCY CONSTRAINTS

Diane L. Peters
Department of Mechanical Engineering
University of Michigan
Ann Arbor, MI 48109
dlpeters@umich.edu

Katsuo Kurabayashi
Department of Mechanical Engineering
University of Michigan
Ann Arbor, MI 48109
katsuo@umich.edu

Panos Y. Papalambros
Department of Mechanical Engineering
University of Michigan
Ann Arbor, MI 48109
pyp@umich.edu

A. Galip Ulsoy
Department of Mechanical Engineering
University of Michigan
Ann Arbor, MI 48109
ulsoy@umich.edu

ABSTRACT

A MEMS actuator and its controller are jointly optimized, both sequentially and simultaneously. The sequential problem is formulated to account for controllability by means of a constraint on the actuator's natural frequency. By varying the frequency constraint, sequential optimization generates a set of designs with significantly increased displacement, compared to the original non-optimized design, and with various settling times. In simultaneous optimization, a non-linearly weighted objective function combines the two objectives, and the relative weights are varied. The tradeoff between the two objectives shows that the use of the frequency constraint serves as an effective surrogate for controllability of the actuator.

INTRODUCTION

Many systems exhibit strong interactions between their static and dynamic characteristics. These interactions present special challenges in the optimal design and control (or, co-design) of such systems. Among these systems are some micro-electrical mechanical system (MEMS) structures, such as the study presented here. MEMS devices are useful in many fields, including biomedical and space systems, due to their small size and low power requirements. A co-design approach, using simultaneous optimization of the artifact, or plant, and its controller is effective in designing coupled systems. However, this is computationally expensive. Sequential formulation of these systems would permit easier solution, as well as offering the advantage that the problem can be decomposed according to the areas of expertise required for solution. By modifying the sequential formulation to account for controllability, it is possible to realize these advantages while obtaining a sufficiently close solution to that found in the simultaneous problem formulation.

It has been demonstrated, both in theoretical work and through a variety of case studies, that the design of an artifact, or plant, and its controller may be coupled. The coupling has been quantified in terms of the weight given to the design and control objectives, and special situations where that coupling does vanish have been described in [1]. Strategies for optimal design of coupled systems have been formulated [1, 2]. Coupling has been studied in the formulation of modeling and controller design problems [3], and has been used in the decomposition of design optimization [4]. Coupling between the plant and controller has been demonstrated to be critical in the proper design of many structural systems with active control [5, 6], particularly in applications with flexible structures [7, 8] such as aerospace applications [9]. It is also critical in a variety of mechatronic systems including machine tools [10], automotive suspensions [11], and elevators [12], as well as many mechanisms subject to feedback control [13-16]. In the following study, interactions between the design objective of maximizing the actuator's range of motion and minimizing the response time have been modeled. Clearly, increasing the range of motion leads to a longer response time.

In the next section, the problem of increasing the actuator's range of motion and decreasing the settling time will be

formulated, both as sequential and simultaneous optimization problems. Results and discussionare presented in the subsequent sections.

PROBLEM FORMULATION

Significant research efforts have been dedicated to the development of MEMS actuators for out-of-plane motion [17-19]. These actuators have been proposed for applications such as instrumentation for studying biological systems. The particular MEMS device that is the subject of this study has been proposed for a confocal scanning microscope to study biological phenomena that occur on a microsecond timescale [17].

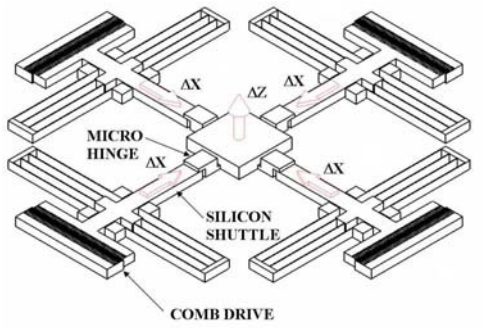

FIGURE 1: ACTUATOR CONFIGURATION

This actuator, as shown in Fig. 1, utilizes four electrostatic comb-drive actuators to produce an out-of-plane displacement. In order to produce this displacement, each of the four comb drives is excited with a voltage, resulting in horizontal movement (ΔX) of the silicon shuttles. The micro-hinges on the polydimethyl siloxane (PDMS) platform bend as shown in Fig. 2, and the platform moves vertically (ΔZ). The amount of movement resulting from the comb drives' actuation depends on both the applied voltage and the physical dimensions of the actuator.

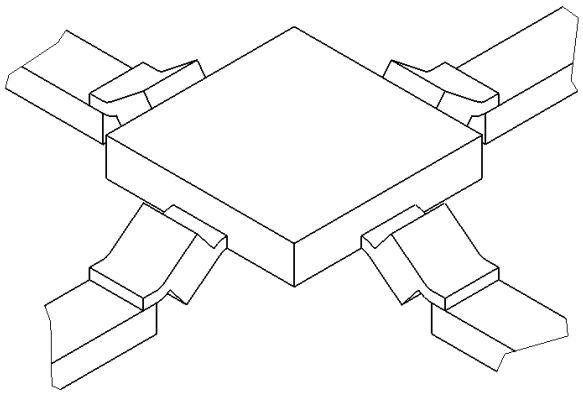

FIGURE 2: HINGE ACTUATION

Sequential Problem

In the sequential optimization problem, the actuator designed by Tung and Kurabayashi, shown in Fig. 1, is first optimized for maximum displacement ΔZ, followed by optimization of its controller for minimum settling time.

The first optimization is formulated with four decision variables. These are the micro-hinge dimensions t, p, h_1, and h_2, as shown in Fig. 3.

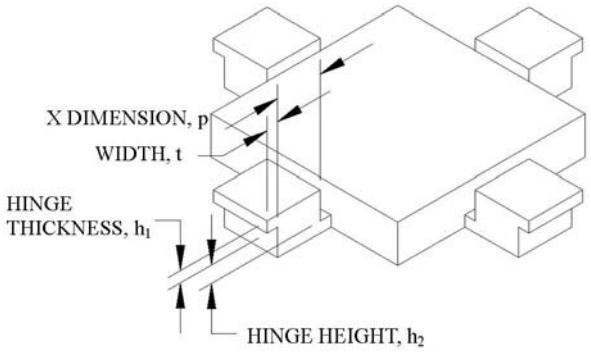

FIGURE 3: MICRO-HINGE STRUCTURE

The design optimization problem is given by (1), also described in detail in [17].

$$\begin{aligned} &\textit{Maximize } f = \Delta Z = (h_1 + h_2)(1-\cos\Delta\theta) + (t+p)\sin\Delta\theta \\ &\textit{Subject to} \\ &g(h_1, h_2, t, p, \Delta\theta, P, N) \le 0 \end{aligned} \tag{1}$$

where $\Delta\theta$ is a function of the decision variables, parameters (P), and constants (N). The constraint vector g consists of constraints on manufacturability, stress, kinematics, mechanical and electrical stability, and open-loop natural frequency of the actuator. The natural frequency is constrained to be at least 10% greater than a specified operating frequency, ω_o, for the device. This operating frequency is chosen to be 500 Hz.

The second step in the sequential optimization is carried out to determine the optimal gains for a specified controller structure. In order to achieve steady-state tracking of the command signal, an integral controller with state feedback is chosen, as shown in Fig. 4.

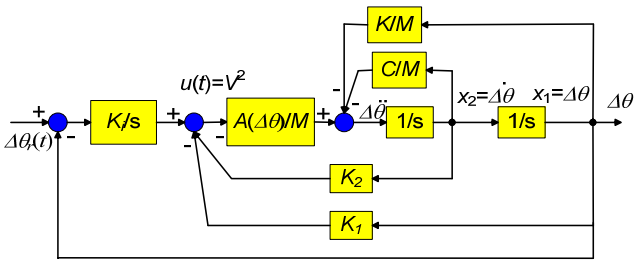

FIGURE 4: SYSTEM DYNAMICS AND CONTROLLER STRUCTURE

The dynamics of the uncontrolled actuator are described by the second-order differential equation

$$M\Delta\ddot{\theta} + C\Delta\dot{\theta} + K\Delta\theta = A(\Delta\theta)V^2 \tag{2}$$

where M is a function of the masses of the platform and shuttle, C represents the damping characteristics of the hinge, and K comes from the stiffness of the hinge and the silicon leaf springs in the comb drive. Note that A is a function of $\Delta\theta$, so the Eq. (2) is nonlinear. The controlled actuator dynamics, as shown in the block diagram in Fig. 4, are described by

$$M\Delta\ddot{\theta} + (C + K_2 A(\Delta\theta))\Delta\dot{\theta} + (K + K_1 A(\Delta\theta))\Delta\theta + K_i A(\Delta\theta)\int_{t=0}^{t_f}(\Delta\theta_r - \Delta\theta)dt = 0 \tag{3}$$

where $\Delta\theta_r$ is the reference signal for the system. The angle $\Delta\theta$ is related to the desired output ΔZ through (1). The three controller gains K_1, K_2, and K_i are the decision variables for the controller optimization. The reference signal is a step input, with a magnitude corresponding to the maximum ΔZ found in the first optimization. The objective function is the 1% settling time t_s, as determined by a Simulink simulation of the system.

Minimize
$$f = t_s$$
Subject to (4)
$$g(K_1, K_2, K_i, P, N) \le 0$$

The constraints are based on the requirement that all gains be positive, that the system overshoot should be 5% or less, and that the control effort available to the system is limited to 25 volts. The decision variables from the first optimization are treated as parameters in the control optimization. It is assumed that the angle $\Delta\theta$ is measured.

Parametric Study of Sequential Problem

In the sequential problem formulation, the constraint on the natural frequency of the actuator is active; thus, the optimum is a function of the operating frequency, ω_o. By varying this constraint, different designs are produced. The specified operating frequency, ω_o, for the actuator is varied from 500 Hz to 2500 Hz in the first part of the sequential formulation. The optimization for maximum displacement is repeated, and the controller gains are optimized for each of these designs.

Simultaneous Problem

The simultaneous problem is formulated as a single objective function with seven decision variables. Evaluation of sample design points showed that the Pareto set is not convex, and therefore the objective is formulated using an exponential weighted criteria function [20]. This objective function is formulated in Eq. (5), with weight W ranging from 0 to 1. Higher weights mean more importance is given to the actuator's range of motion, and lower weights give more importance to the settling time.

Minimize
$$f = \left(e^{mW} - 1\right)e^{-m\Delta Z} + \left(e^{m(1-W)} - 1\right)e^{mt_s}$$
Subject to: (5)
$$g(h_1, h_2, t, p, K_1, K_2, K_i, \Delta\theta, P, N) \le 0$$

The constraints for the simultaneous problem consist of the combined set of constraints from the two parts of the sequential problem, with one modification. In the simultaneous problem, the constraint on the natural frequency of the system is eliminated, and instead the frequency of the controlled response is constrained.

RESULTS

Sequential Problem

In the first portion of the sequential problem, the value of ΔZ increased from 0.95 μm in the original design to 6.79 μm in the new design. This represents an increase in the range by a factor of more than seven. The changes in the decision variables are shown in Table 1. At these values, the frequency constraint and two of the manufacturing constraints are active.

TABLE 1: COMPARISON OF ORIGINAL AND OPTIMIZED ARTIFACT DESIGNS

	Original Design	Optimized Design
t(μm)	20	30
p(μm)	80	599
h_1(μm)	20	6
h_2(μm)	30	53
ΔZ(μm)	0.95	6.79

It is evident that the hinge dimensions change significantly; in particular, the overall length of the hinge increases, producing the

design shown in Fig. 5. It is expected that, since this design is not as stiff as the original configuration, it will present a greater challenge to the controller.

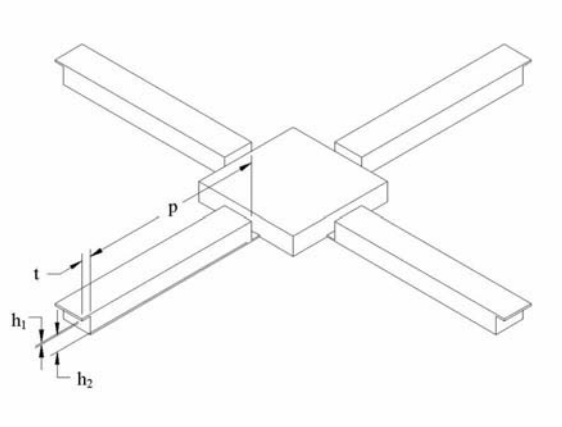

FIGURE 5: CONFIGURATION OF OPTIMIZED MICRO-HINGE

In the second part of the problem, the controller optimization yielded a settling time of 0.568 ms. An optimal set of gains for the original design yielded a settling time of 0.208 ms. The optimal values of the gains for both designs are given in Table 2. At these values, the constraint on the maximum control effort is weakly active. [21]

TABLE 2: COMPARISON OF CONTROL GAINS FOR ORIGINAL AND OPTIMIZED DESIGNS

	Original Design	Optimized Design
K_1	93342	401085
K_2	4.9831	48.374
K_i	1.3032×10^9	1.5421×10^9
t_s (ms)	0.208	0.568

It can be seen that the optimal gains for the new design are higher than the gains for the original design. The settling time is also higher for the new design than for the original one, indicating that the two goals of maximizing displacement and minimizing settling time are in competition with one another.

The angular position of the hinge for both the original and optimized designs is shown in Fig. 6. The responses are normalized with respect to the steady-state value, which is dependent upon the values of the decision variables found in the first optimization. The response of the original design is represented by the dashed line, and the response of the optimized design is represented by the solid line.

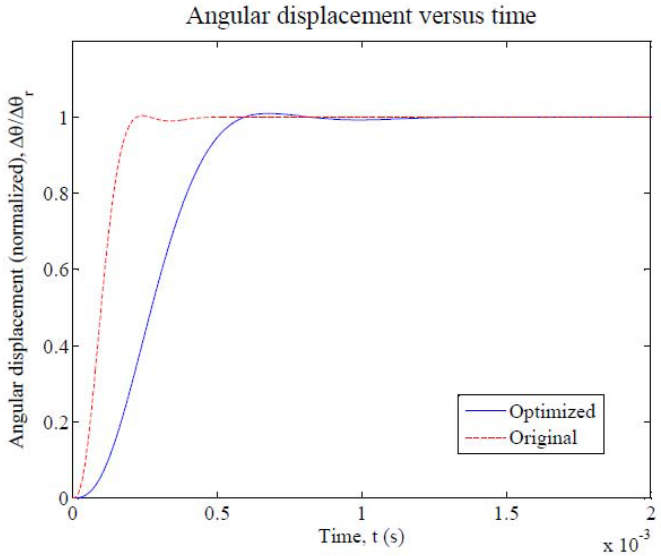

FIGURE 6: DISPLACEMENT RESPONSE OF SYSTEM

The voltage requirement is shown in Fig. 7. The effort needed to control the optimized design is greater than that required for the original design. Again, the dashed line represents the original system, and the solid line denotes the optimized system.

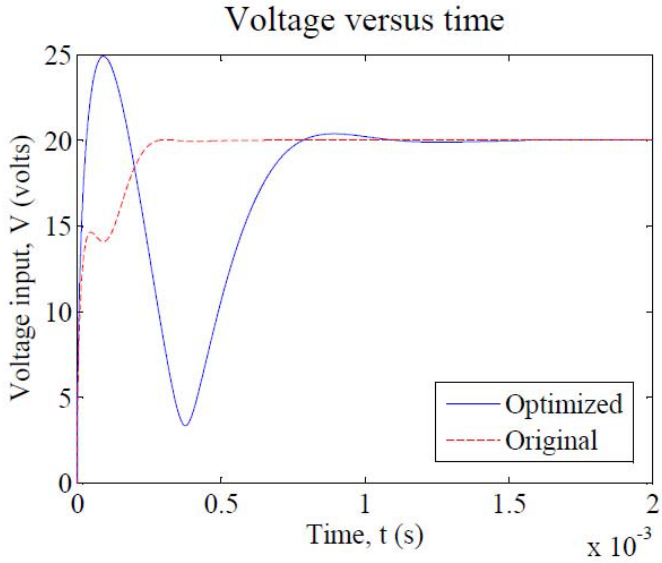

FIGURE 7: CONTROL EFFORT FOR SYSTEM

Parametric Study of Natural Frequency

In the first part of the sequential problem, the natural frequency of the actuator is constrained to be at least 10% greater

than the desired operating frequency, ω_o, of the actuator. As the specified operating frequency is varied, different solutions are obtained for the maximum displacement and the corresponding minimum settling time. Higher operating frequencies produced lower range of motion, but had a lower settling time as well. The mechanical designs generated by the parametric study are given in Table 3; controller gains for each design are given in Table 4; and the relation between ΔZ and t_s is shown in Fig. 8.

TABLE 3: OPTIMIZED ARTIFACT DESIGNS FOR VARYING ω_O

ω_o (Hz)	h_1 (μm)	h_2 (μm)	t (μm)	p (μm)	ΔZ (μm)
500	6	53	30	599	6.79
750	6	51	30	400	4.93
1000	6	51	30	296	3.84
1250	6	52	30	234	3.11
1500	6	52	30	189	2.57
1750	6	54	30	155	2.15
2000	6	54	30	126	1.80
2250	6	54	30	100	1.50
2500	6	53	30	73	1.23

Varying the operating frequency has a large effect on the dimension p of the micro-hinge. This dimension has considerably smaller values when the operating frequency is large, which corresponds to a stiffer system. This also corresponds to smaller values of the maximum displacement, with ΔZ ranging from 6.79 to 1.23.

TABLE 4: OPTIMIZED CONTROLLER DESIGNS FOR VARYING ω_O

ω_o (Hz)	K_1	K_2	K_i	t_s (ms)
500	401085	48.3743	1.5421×10^9	0.568
750	361579	34.4323	1.8102×10^9	0.470
1000	301556	23.7218	1.8725×10^9	0.387
1250	287850	15.3381	2.5500×10^9	0.248
1500	312158	13.3856	3.3879×10^9	0.201
1750	286991	11.1882	3.4939×10^9	0.182
2000	253074	9.1044	3.4002×10^9	0.166
2250	236230	8.1676	3.4074×10^9	0.158
2500	216505	6.7633	3.4629×10^9	0.142

As the operating frequency is increased, the settling time decreased, with t_s ranging from 0.568 ms to 0.142 ms. All of these designs have a larger maximum displacement than the original design (shown as a dark circle in Fig. 8), and five of them match or improve the settling time.

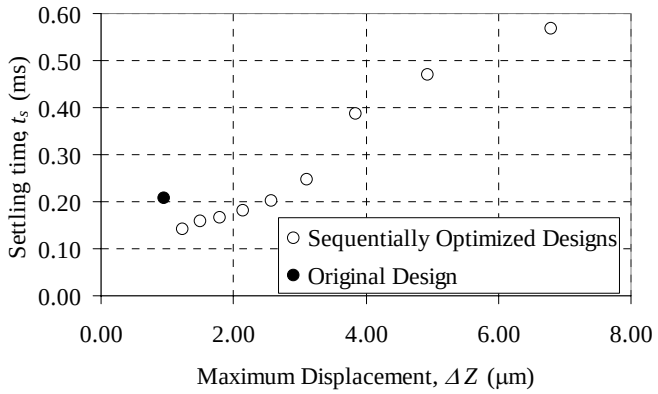

FIGURE 8: SETTLING TIME VS. DISPLACEMENT FOR VARYING ω_O SEQUENTIALLY OPTIMIZED DESIGNS (○), AND COMPARISON TO ORIGINAL DESIGN (●)

The responses of the designs found are shown in Figs. 9 and 10. In all cases, the overshoot is well within the 5% constraint. There is a clear shift in the response as the operating frequency is increased, with a higher operating frequency corresponding to a rapid rise in the displacement.

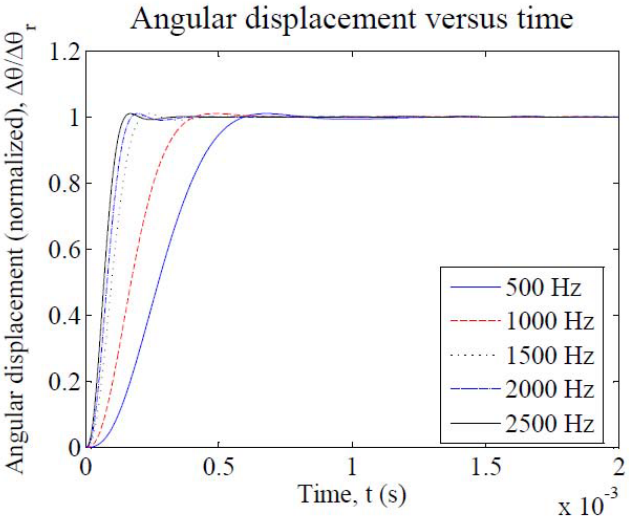

FIGURE 9: DISPLACEMENT RESPONSES FOR VARYING ω_O FOR THE SEQUENTIALLY OPTIMIZED DESIGNS

In Fig. 10, the maximum control effort tends to decrease with increases in the operating frequency. Also, for higher operating frequencies, the fluctuations are not as large as for the lower frequencies, and the effort reaches its steady-state value more quickly. This indicates that, as expected, the stiffer designs produced by a greater value of the operating frequency present a greater ease of control, but achieve reduced maximum displacements.

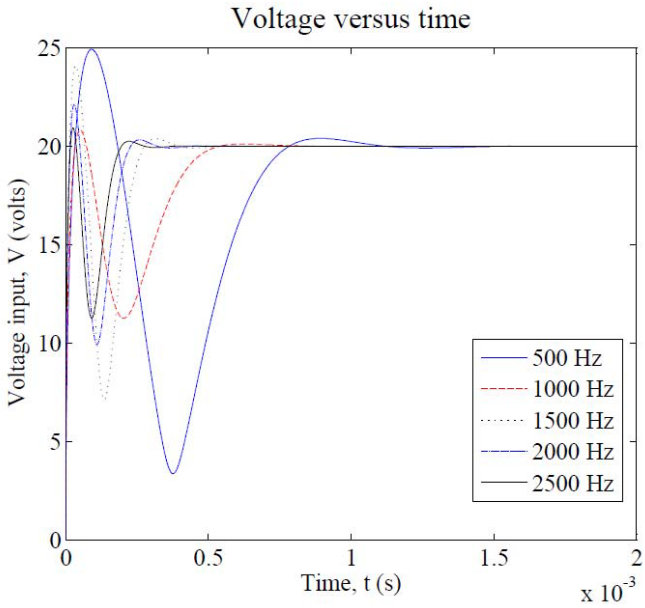

FIGURE 10: CONTROL EFFORT FOR VARYING ω_O FOR THE SEQUENTIALLY OPTIMIZED DESIGNS

Simultaneous Problem

The tradeoff between the design and control objectives is shown in Fig. 11. These results confirm that the two objectives compete, and that increasing the range of motion of the actuator will set limits on the performance of the actuator under control.

Larger values of W produced designs in which manufacturability constraints are active. No constraint activity is evident at lower values of W.

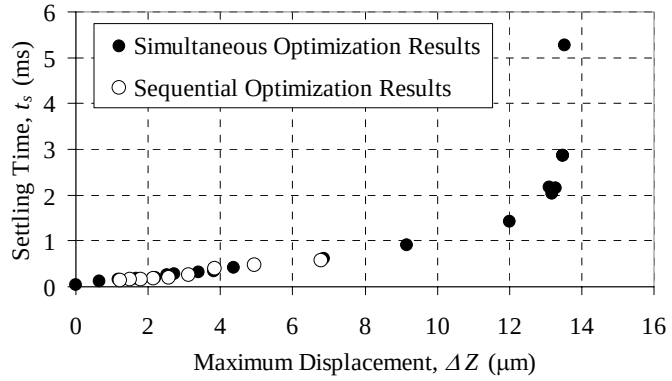

FIGURE 11: COMPARISON OF SIMULTANEOUS (●) AND SEQUENTIAL (○) OPTIMIZATION RESULTS

DISCUSSION

The physical dimensions of the actuator and the controller gains are clearly quite different in the two problem solutions. In the sequential problem, for each value of ω_o, the actuator has a long, thin configuration. In the simultaneous problem, the resulting configurations vary considerably, with some of them long and thin and others considerably thicker. Despite these differences, the solutions found in the sequential problem constrained by the natural frequency of the actuator closely track the Pareto curve generated by the simultaneous problem, as shown in Fig. 11. For a given application, therefore, there may be more than one design available to satisfy the requirements on displacement and settling time. This also indicates that, for this choice of decision variables and controller architecture, either solution method will produce a set of optimal solutions. Each method presents its own advantages and challenges.

The sequential problem offers the advantage of less computational effort. For a typical point, 68 function calls are required for the artifact optimization, and 59 function calls for the control optimization, with only the control optimization involving simulation. By contrast, generation of a typical point for the simultaneous problem requires 137 function calls, all of which require simulation. However, in the sequential formulation, it is not obvious what value of the operating frequency ω_o would yield a particular settling time t_s. Furthermore, there is no way to be certain how much of the Pareto set is included in the sequential solution. The sequential approach also offers an operational advantage, since expertise in the design of the artifact and in controller design may be located in different departments within an organization.

The simultaneous problem, as stated, requires more computational effort. Furthermore, if the Pareto set is non-convex, as in this case, special care must be taken in formulating a combined objective function. A linear combination, which is often used in multi-objective optimization problems, will not generate the full set of Pareto optimal points.

Overall, sequential optimization utilizing the natural frequency to ensure controllability is the preferred method for this problem. It produces a set of optimal designs with less computational effort than the simultaneous solution method. While it would not produce the full set of designs without some tuning of the natural frequency constraint, it does generate a range of designs which could be used in a variety of different applications of the device.

SUMMARY AND CONCLUDING REMARKS

In considering both sequential and simultaneous formulations for the design of a MEMS actuator and its controller, it can be seen that this problem is coupled. In order to achieve optimal results for a given application, it is necessary to consider the coupling. The coupling can be addressed either by including natural frequency as a measure of controllability in a sequential formulation, or by formulating the problem as a simultaneous optimization.

While sequential optimization using the natural frequency as a controllability surrogate is effective for this actuator, this is not true in all cases. In many systems, the natural frequency is a poor predictor of controllability. Future work will evaluate the

conditions under which the natural frequency of a system is an effective surrogate for controllability, and will also study alternative measures of controllability that can be included in a sequential problem formulation.

ACKNOWLEDGEMENTS

The authors are pleased to acknowledge the financial support of the National Science Foundation under Grant # 0625060.

REFERENCES

[1] Fathy, H. K., 2003. Combined Plant and Control Optimization: Theory, Strategies and Applications. *Mechanical Engineering.* Ann Arbor, University of Michigan.

[2] Reyer, J. A., 2000. Combined Embodiment Design and Control Optimization: Effects of Cross-Disciplinary Coupling. *Mechanical Engineering.* Ann Arbor, University of Michigan.

[3] Brusher, G. A., Kabamba, P. T. and Ulsoy, A. G., 1994. "Coupling Between the Modeling and Controller – Design Problems, Part I: Analysis". *ASME Journal of Dynamic Systems, Measurement and Control*, 119, pp. 498-512.

[4] Alyaqout, S. F., Papalambros, P. Y. and Ulsoy, A. G., 2005. "Quantification and Use of System Coupling in Decomposed Design Optimization Problems". *Proceedings of ASME IMECE*, Orlando, FL.

[5] Haftka, R. T., 1990. "Integrated Structure/Control Optimization of Space Structures". *AIAA Journal*, pp. 1-9.

[6] Kosu, R. L., Kabuli, G. M., Morrison, S. and Harn, Y. P., 1990. "Simultaneous Control and Structure Design for Large Space Structures". *American Control Conference.* San Diego, CA.

[7] Kim, Y., Kum, D. and Nam, C., 1997. "Simultaneous Structural/Control Optimum Design of Composite Plate with Piezoelectric Actuators". *Journal of Guidance, Control, and Dynamics*, 20**,** pp. 1111-1117.

[8] Khorrami, F. & Rastegar, J. S., 1995. "Simultaneous Structure and Control Design for a Flexible Pointing System Actuated by Active Materials". *34th Conference on Decision & Control.* New Orleans, LA.

[9] Kajiwara, I. and Haftka, R. T., 2000. "Integrated Design of Aerodynamics and Control System for Micro Air Vehicles". *JSME International Journal*, 43.

[10] Chen, C.-Y. & Cheng, C.-C., 2005. "Integrated Design for a Mechatronic Feed Drive System of Machine Tools". *IEEE/ASME International Conference on Advanced Intelligent Mechatronics.* Monterey, CA.

[11] Fathy, H. K., Hrovat, D., Papalambros, P. Y. and Ulsoy, A. G., 2003. "Nested plant/controller optimization and its application to combined passive/active automotive suspensions". *American Control Conference.* Denver, CO.

[12] Fathy, H. K., Bortoff, S. A., Copeland, G. S., Papalambros, P. Y. and Ulsoy, A. G., 2002. "Nested Optimization of an Elevator and its Gain-Scheduled LQG Controller". *ASME IMECE2002*. New Orleans, LA.

[13] Zhang, W. J., Li, Q. and Guo, L. S., 1999. "Integrated Design of Mechanical Structure and Control Algorithm for a Programmable Four-Bar Linkage". *IEEE/ASME Transactions on Mechatronics,* 4**,** pp. 354-362.

[14] Tilbury, D. M. and Kota, S., 1999. "Integrated Machine and Control Design for Reconfigurable Machine Tools". *IEEE/ASME International Conference on Advanced Intelligent Mechatronics.* Atlanta, GA.

[15] Wan, J., Li, Q. and Wu, F. X., 2002. "Integrated Design and Control of a Closed-chain Mechanism". *Seventh International Conference on Control, Automation, Robotics and Vision.* Singapore.

[16] Ravichandran, T., Wang, D. and Heppler, G.., 2006. "Simultaneous plant-controller design optimization of a two-link planar manipulator". *Mechatronics,* 16**,** pp. 233-242.

[17] Tung, Y.-C. and Kurabayashi, K., 2005. "A Single-Layer PDMS-on-Silicon Hybrid Microactuator With Multi-Axis Out-of-Plane Motion Capabilities - Part I: Design and Analysis". *Journal of Microelectromechanical Systems*, 14**,** pp. 548-557.

[18] Kim, C.-H. and Kim, Y.-K., 1999. "Integration of a microlens on a micro XY-stage". *Proceedings of Device and Process Technologies for MEMS and Microelectronics*, Gold Coast, Australia.

[19] Sun, Y., Piyabongkarn, D., Sezen, A., Nelson, B. J., and Rajamani, R., 2002. "A high-aspect-ratio two-axis electrostatic microactuator with extended travel range". *Sens. Actuators A: Phys*., 102, pp. 49-60.

[20] Athan, T. W., 1994. "A Quasi-Monte Carlo Method for Multicriteria Optimization". *Mechanical Engineering.* Ann Arbor, University of Michigan.

[21] Pomrehn, L. P. and Papalambros, P. Y., 1994. "Global and Discrete Constraint Activity". *Journal of Mechanical Design*, 116, pp. 745-748.